UDC 621.224.6-752

VIBRATION REDUCTION OF REVERSIBLE PUMP-TURBINES

Tsuneo Ueda

Takashi Kubota

Hiroyuki Aoki

Kawasaki Factory

I. INTRODUCTION

Because of large head variation from 100 m to 50 m in the Hatanagi No. 1 pumped storage power plant which was placed on service in 1962 as one of the largest pumped storage power plants in Japan at that time, vibration occurred in pumping at high head and generating at low head. It was desired to improve the high head operation more efficient and stable in order to increase the operating efficiency of the pumped storage plant even though there has been some sacrifice of low head operation. Therefore, improved impeller-runners have been developed intended mainly for improvement of high head pumping performance, especially for reduction of vibration resulting from back flow at the pump inlet. The stationary parts excluding impeller-runner have not been changed at all and only the vane shape of the impeller-runner have been changed to improve performance and reduce vibrations. This approach was carried out in the following steps.

1. On the basis of 10 years operating experience at site, the problem points were examined in respect to the hydraulic performance and vibration of the pump-turbine.
2. A large scale model completely similar to the prototype was newly manufactured and model tests were performed to confirm the problems points at site mentioned above in the Fuji hydraulic laboratory.
3. The site and model tests were compared and the effectiveness of the model vibration test was verified.
4. A thorough model vibration test including four quadrant characteristics was performed and the criteria for evaluating the effects of the improved impeller-runners to be developed were established.
5. The vane shape of the original impeller-runner was analyzed hydraulically using Fuji computer program and the improved impeller-runner development policies were established on the basis of a study of the correlation between the above-mentioned problem points at site and the vane design parameters and an investigation of optimum matching of impeller- runner characteristics with the hydraulic performance of the wicket gates and stay vanes.
6. Various vane design parameters were selected, many new improved impeller-runners were designed by Fuji computer program. Four models selected out of many designs were manufactured, successive model tests were performed and the best runner was finally selected.
7. Using the results of the model tests, simulation calculation of the transient phenomena as well as the steady state operation of the prototype was performed by Fuji computer program and comparisons were made with the present impeller-runner. It was confirmed that the newly developed impeller-runner was better under all conditions.

Several topics from the above mentioned approaches will be explained in the sections below.

II. SUMMARY OF PROTOTYPE PUMP-TURBINE OPERATING EXPERIENCE

A summary was made of the 10 years of operating experience as a background for the development of the improved impeller-runner. Problem points were examined and the development policy was clarified.

1. High Head Operation

The No. 1 unit of the Hatanagi No. 1 pumped storage power plant first went into service in September, 1962 employing an Allis-Chalmers pump-turbine (max. output : 51,800 kW) and a Fuji Electric generator-motor (58,880 kVA). *Fig. 1* shows the operating experience at various heads from the start. As can be seen from the figure, operation at $H=$ 70 m or less was only 16% for pumping and 10% for generating so that the operating hours at low heads were very few. On the contrary, high head operation at $H=90$ m or over was 50% for generating and 16% for pumping but this was because pumping at 95 m or over was avoided as much as possible due to vibrations as will be described in the next section. So the experience with high head operation was actually great for both pumping and generating.

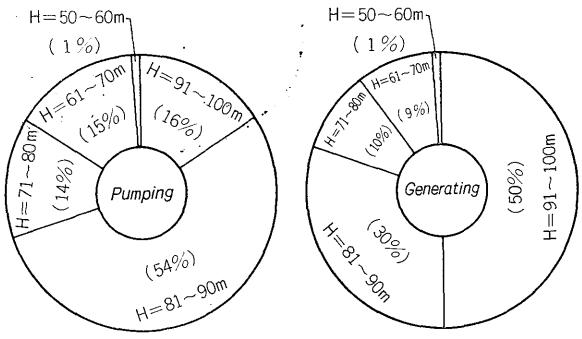

(a) Pumping (b) Generating

Fig. 1 Percentage of operating hours at various head

Therefore, the improvement of characteristics at high head operation and in particular reduction of vibration at maximum head pumping are very desirable in practice.

2. Partial Load Generating

Of the total generating hours, there has been a considerable amount of partial load operation in recent years as can be seen from *Fig. 2* which indicates operation percentages at various generating modes. Partial load operation has been more than six times that of full load operation. Therefore, it is especially desirable to improve partial load performance even at high head generating.

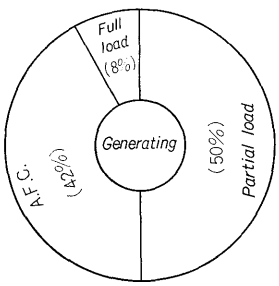

Fig. 2 Percentage of operating hours at various generating modes

3. Pump Input Power

The maximum input power as pump of the Francis pump-turbine is generally required at low head and the maximum generating output power is obtained at maximum head. Therefore, when the head variation is large, the input power at maximum head pumping becomes very low when compared with generating output power, and this is undesirable from the standpoint of the capacity absorbed surplus energy during the night. In the case of the Hatanagi plant, the maximum generating output is 51,800 kW while the pumping input is only 34,200 kW at a high head of $H=95$ m. Thus, it is desirable to increase the pumping input at higher heads.

4. Cavitation

Cavitation pitting developed on the suction surface of the vanes at the impeller inlet during high head pumping. Therefore, in cases of increasing the pumping hours at high heads, it is necessary to consider suppression of cavitation at the same time. Cavitation pitting developed on the suction surface of the bucket at the runner entrance during full load generating at maximum head. Suppression of this cavitation is also required.

III. COMPARATIVE TEST OF PROTOTYPE AND MODEL

1. Pumping Cycle

From the operating experience obtained so far with the prototype, it has been confirmed that vibrations increase from heads near $H=95$ m. From the vibration tests on the prototype conducted recently at the site, the solid lines in *Fig. 3* show the typical results of measurements of hydraulic pressure fluctuation at heads of $H=90.5$ m and 95.0 m. The magnitude of the pressure fluctuation at the position between the impeller-runner and wicket gates so called priming pressure fluctuation was measured for various degrees of gate opening. At $H=90.5$ m (*Fig. 3* (a)), the pressure fluctuations are small and the stable operating range is wide. The pressure fluctuation reaches a peak after the gate opening becomes rather small. However, when $H=95.0$ m (*Fig. 3* (b)), the range of the valley in the pressure

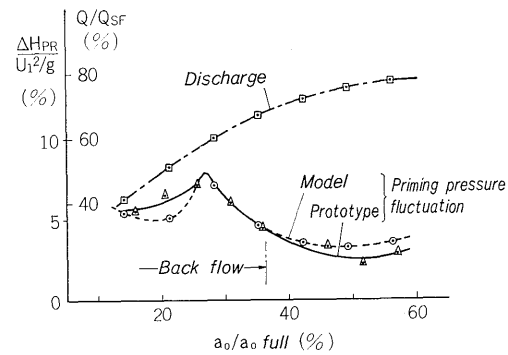

(a) H=90.5 m

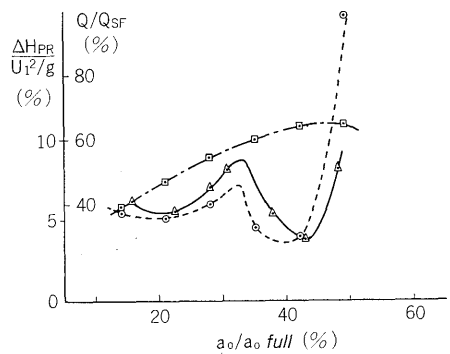

(b) H=95.0 m

Fig. 3 Pressure fluctuation characteristics at high head pumping

fluctuation curve becomes narrow and the value at the bottom of the valley is about twice that in the case of the 90.5 m head and stable operation with small

vibrations becomes impossible. The pumping discharge when the pressure fluctuations reach a peak is about the same in both figures and it suggests the vibrations are highly concerned with the discharge.

The vibrations at high head pumping (or small discharge) were assumed to be caused by back flow from the impeller inlet. Therefore, a new model completely similar to the prototype was manufactured and model retesting was performed (hereafter, this model will be referred to as the A-runner). The broken lines in *Fig. 3* show an example of the results of model vibration test performed at a test head of 1/2 the actual head using a large scale model with an impeller vane outer diameter of 500 mm. There is a high degree of coincidence with the prototype test results. The effectiveness of the model vibration tests was verified clearly and satisfactorily including the measurements of hydraulic pressure fluctuations at other positions as well as above mentioned priming pressure fluctuation, wicket gate hydraulic torque fluctuations, cavitation noise and visual observations of the flow pattern.

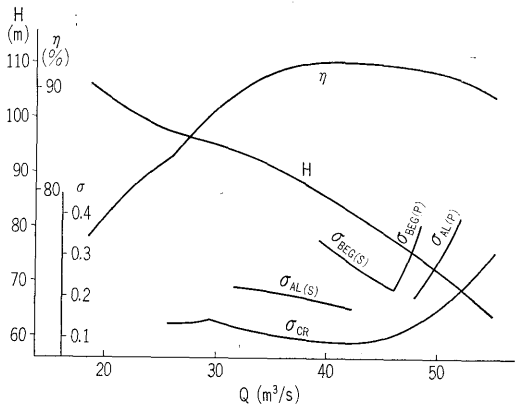

Fig. 4 Pump performance

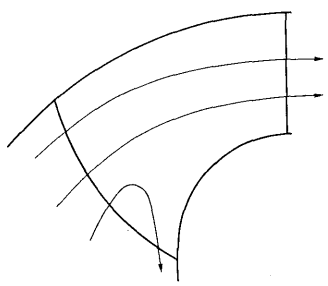

Fig. 5 Flow pattern of back flow as pump

Fig. 4 shows the model pump performance obtained. Stall phenomena (flow separation from vane suction surface) are observed visually to begin from the shroud side of the impeller vane inlet as pump from a small discharge corresponding to $H=93$ m. From a smaller discharge equivalent to 94 m, the part of water which was once sucked between the vanes starts to reverse back in the upstream direction against the main flow (*Fig. 5*), and the hydraulic pressure fluctuations, noise, etc. reached a maximum in the

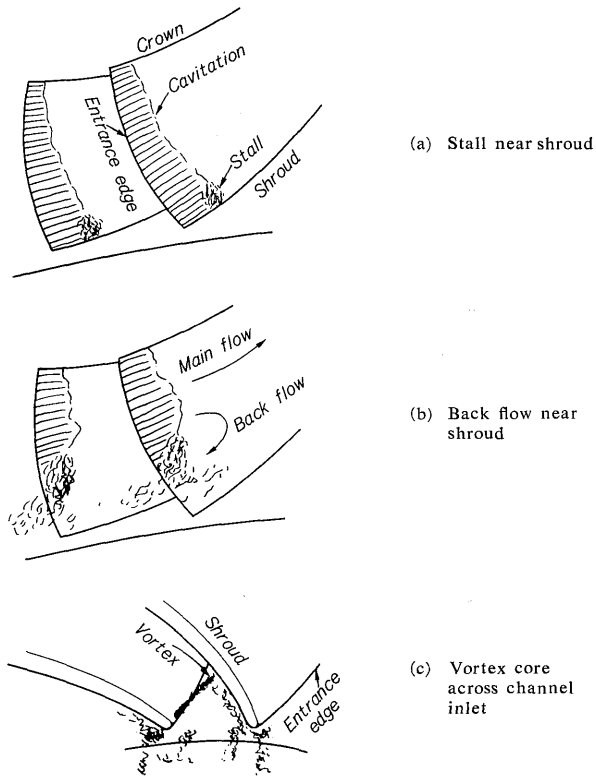

Fig. 6 Flow pattern at pump inlet (suction surface)

vicinity of 97 m. Back flow can be detected quantitatively by measuring the noise and hydraulic pressure fluctuation but first the cavitation developed on the vane suction surface becomes unstable (stall) as in *Fig. 6* (a) and then the crack-type cavitation tore off from the vane surface starts to flow away upstream in a flush like manner (back flow) in *Fig. 6* (b) with the decreased discharge. When the discharge becomes further small, vortices occur almost perpendicular from the vane surface near shroud across the channel inlet in the vent direction and vibration becomes peak. These vortices could be clearly observed visually by the light of stroboscope in *Fig. 6* (c). As is evident from the head-discharge curve (*Fig. 4*), the shape of the curve is normal at $H=93$ m or less which suggests the flow pattern in the impeller is stable. However, at 98 m or above, the effect of secondary radial flow in the impeller inlet becomes dominant and the gradient of the head-discharge curve increases. It is evident that the vibration zone of back flow just corresponds to the transition zone of the two curves. The discharge Q_{BF} to begin back flow is measured to be 68% of the discharge Q_{SF} at the shock free entry point in respect to the impeller vane inlet near shroud and the original impeller-runner (A-runner) can be said to have the usual back flow characteristics for this specific speed compared with the many experimental experience in Fuji Hydraulic laboratory[1].

As was shown in *Fig. 4*, cavitation occurs on the suction surface of the vane inlet at $H=78$ m or over. Since the present prototype impeller-runner is of carbon steel casting, some repair overlays of the

cavitation damage have been performed in the past. The shape of the cavitation area of the model was confirmed by visual observation to be extremely similar to that of the repaired area. In the case of the A-runner, the attack angle of the vane at the impeller inlet is somewhat changed between crown and shroud so that unusual cavitation occurs from the lower head (large discharge) near crown. It was also observed that even in the vibration zone, the cavitation near crown remains without blowing away due to back flow because of above-mentioned difference of vane inlet attack angles.

2. Generating Cycle

In the case of generating mode, vibrations occur in the low head range of 65 m or less. *Fig. 7* shows the relation between the mussel curves and the pressure fluctuations as typical example of the model vibration test results. When the flow incidence angle for the runner bucket with the low head operation becomes too small (the negative value is too large), the flow separates from the bucket pressure surface and severe vibration arises as can be seen in the figure.

On the other hand, from the standpoint of the power network control function of the pumped storage power plant, stable operation during partial load (reserve operation) becomes important. *Fig. 8* shows an example of the priming pressure fluctuation at $H=90.3$ m. Generally in a straight turbine, surging develops caused by the eccentricity of the forced vortex core occurred at runner outlet when the discharge decreases about 40~70% of the optimum discharge without whirl in the runner exit[2]. However, in this A-runner, there is almost no surging and stable operation is possible up to 20% (10 MW) of the maximum output (51.8 MW).

3. Transient State

It was found in the prototype that when there is load rejection from near the full load, and the servomotor stroke of the distributor is reduced to about 20%, the wicket gate does not close after this for a while (stagnation of wicket gate closure) (S-curve in *Fig. 9*). Digital computer simulation was performed in the transient phenomena using the results of the model vibration test including the measurement of the wicket gate hydraulic torque and its fluctuation in the energy dissipation zone (exceeding runaway) and the reverse rpm pump zone. The results indicate that the runner enters into the reverse rpm pump zone (negative disharge shown by the hatched area in *Fig. 9*) at 7 seconds after load rejection and a large opening torque operates in the wicket gates as can be seen in *Fig. 10*. It was also confirmed that severe pressure fluctuations and wicket gate hydraulic torque fluctuations occur simultaneously. Therefore, it was found that the above stagnation phenomenon is caused by a increase in the large opening torque in the reverse rpm pump zone.

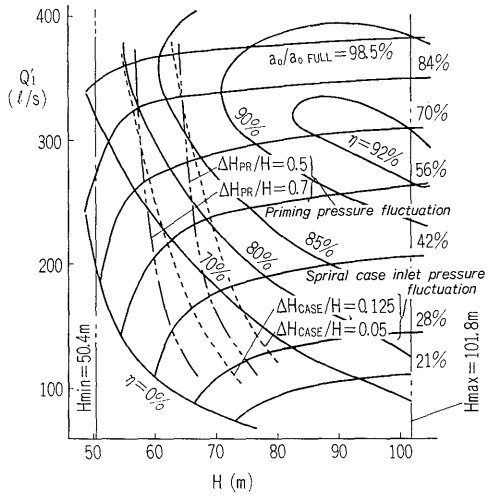

Fig. 7 Correlation of mussel curve and pressure fluctuation at turbining

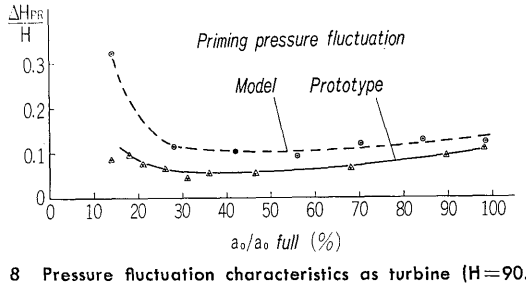

Fig. 8 Pressure fluctuation characteristics as turbine (H=90.3 m)

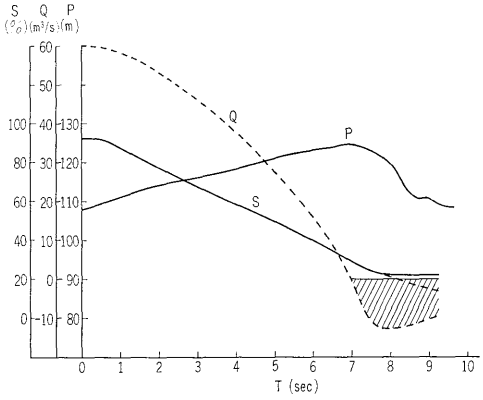

Fig. 9 Load rejection characteristics

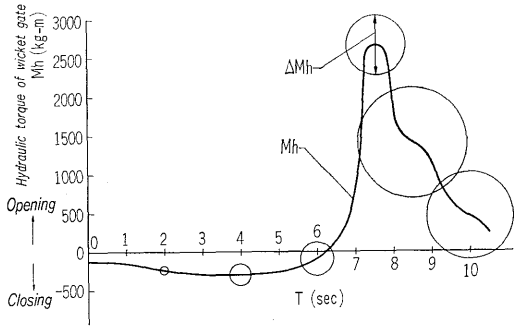

Fig. 10 Wicket gate hydraulic torque at load rejection

IV. DEVELOPMENT OF IMPROVED IMPELLER-RUNNER

1. Shape of Impeller-runner

In order to develop an impeller-runner with improved characteristics, the following design parameters were selected and four new model impeller-runners were manufactured. Below, these four are refered to as the B, C, C_1 and D-runners. However, only the C_1-runner is the modified one from the C-runner by revising the vane shape at outer diameter. *Fig. 11* shows photos of the A, B, C_1 and D-runners.

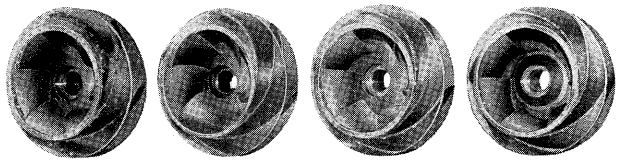

(a) A-runner (b) B-runner (c) C_1-runner (d) D-runner

Fig. 11 Photos of developed model impeller-runners

1) Impeller inlet

(1) Vane inlet angle

Generally, the ratio of the discharge Q_{BF} at the beginning of the back flow to the discharge Q_{SF} at the shock free entrance of flow into the impeller-vane (as pump) tends to be almost constant irrespective of the specific speed if the impeller-runner is designed based on the same criteria[1]. Therefore, in order to shift the vibration zone to the smaller discharge, it is highly effective to decrease the vane inlet angle of the impeller in such a way that Q_{SF} and therefore Q_{BF} becomes small. As a result, the pump characteristics are almost unchanged (since only the pump inlet part is changed), cavitation on the vane suction surface of the impeller inlet can be suppressed and therefore, stall and back flow can also be shifted to the smaller discharge. On the contrary, it is easy for cavitation to occur from the pressure surface at large discharges. Since there is a tendency for the runner discharge vent as turbine to become narrow as the result of the reduction of the vane inlet angle (*Fig. 12*), the optimum efficiency point as turbine tends toward a small discharge and the partial load efficiency can be improved but conversely the efficiency at full load tends to decrease. Considering the above mentioned points, a comparison of the impeller inlet angle sa pump near shroud of the selected impeller-runners is shown in *Table 1*.

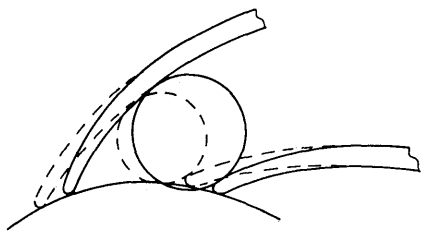

Fig. 12 Relation between vane angle and vent at turbine discharge

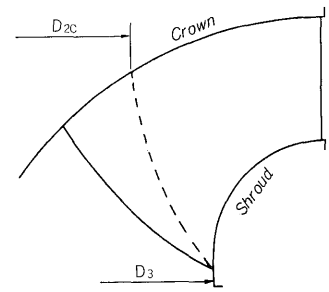

Fig. 13 Minimum inner diameter of vanes near crown

Table 1 **Comparison of design parameters of runner vane**

			A	B	C	C_1	D
Vane inlet angle (pump)	$\beta_2-\beta_{2(A)}$	deg	—	-3	-3	-3	-3.4
Min. I.D. of vanes (near crown)	D_{2c}/D_3	%	51	36	54	54	65
Max. O.D. of vanes	$(D_1-D_{1(A)})/D_{1(A)}$	%	—	0	1.7	0.65	1.7

(2) Vane inlet diameter near crown

Generally the back flow phenomena at pump inlet is greatest in an axial flow pump and there is a tendency for the back flow to decrease to occur in mixed flow and difficult to occur in radial pumps. When the vane inlet diameter near crown (D_{2c} in *Fig. 13*) is small in respect to the edge diameter of the impeller D_3. In Francis type pump-turbines (i.e. the vane near crown is extended toward the pump inlet), the impeller becomes to be analogous to the axial flow type. Therefore, the radial flow in the impeller inlet becomes large with reduced discharge and back flow occurs easily (*Fig. 5*). Conversely, when the vane inlet diameter near crown D_{2c} is rather large in respect to the eye diameter of the impeller D_3 (broken line in *Fig. 13*), back flow occurs with difficulty since the contour of the vane inlet is alike to the radial flow type.

Since the peripheral speed is high with the larger D_{2c} there is a disadvantage in that it is easy for cavitation at the vane inlet near crown to occur. In addition, it is also easy for whirl flow to occur at the runner exit during turbining so that the efficiencies and vibrations at both partial and full load become inferior (variable discharge performance deteriorates). Careful considerations must be taken for the selection of D_{2c}/D_3 because of these tendencies.

The relation between the back flow of pumping and the value of D_{2c}/D_3 has been pointed out previously by some investigators but there are actually suprisingly few published papers[3] on the experimental examples and there are almost none concerning the effect of D_{2c}/D_3 on the pump-turbine performance mentioned above. In the experimental researchs on

pump-turbines conducted so far by Fuji Hydraulic Loboratory, the influence of the magnitude of D_{2c}/D_3 has been confirmed for some groups of impeller-runners of various specific speeds. In this case, it was selected as one of the most important design parameters. *Table 1* and *Fig. 11* show comparisons of the D_{2c}/D_3 for each impeller. In order to confirm the effects of D_{2c}/D_3 quantitatively the D_{2c} of B runner was selected deliberately small value.

(3) Vane angle distribution near shroud

As can be seen in *Fig. 12*, it is usual for the vane angle β to increase gradually from the vane inlet to the channel inlet (position across vent) along the stream-line near shroud, in order to decrease the vane inlet angle as pump and yet enlarge the discharge vent as turbine as much as possible. As was mentioned previously in clause 1 of chapter III, the discharge at the beginning of back flow of the pump inlet is closely related to the flow separation from the impeller vane suction surface (especially near shroud). Therefore, special consideration has been paid so that the cavitation and back flow are suppressed as much as possible with the reduction of rate of change of vane angle along the shroud. *Fig. 14* shows a comparison of the vane angle distribution. Since the vane inlet angle as pump in the A-runner is too large, the cavitation characteristics tend toward a larger discharge.

2) Impeller outlet

(1) Max. outer diameter of impeller vanes

In cases where only the max. outer diameter D_1 in the same impellers were large, both head and discharge increase proportionally to D_1^2 and the pump input power increases in proportion to D_1^4. For example, if D_1 becomes 1% larger, the head and discharge both increase by 2% and the pump input power increases by 4%. However, since the back flow is exclusively affected by the vane shape of the pump inlet, there will be almost no change in the discharge at the beginning of back flow even when D_1 increases. Therefore, the head rise with increase of D_1 for the same discharge can be explained as shown in *Fig. 15*. In other words, the ratio of the discharge change rate to the head change rate[1] of this impeller is $G_{Q/H} \equiv (\Delta Q/Q)/(\Delta H/H) \fallingdotseq 2.7$ at the higher head. Therefore, as is evident from *Fig. 15*, when D_1 is increased by 1%, the head increases by $\Delta H + \Delta Q/G_{Q/H} = 2 + 2/2.7 = 2.7\%$ at the same discharge. By increasing the max. O.D. of vanes D_1 in this way, it is possible to raise the pump input power and at the same time increase the head.

However, in the turbining cycle, the velocity triangle at the bucket inlet changes as shown in *Fig. 16* at the same discharge and wicket gate opening and the low head characteristics are reduced. When D_1 is too large, the space between D_1 and the trailing edge of the wicket gate at max. gate opening becomes too small and there is a danger of vibrations occurring due to interference. Therefore, careful investigations including the problem of strength are necessary to stretch out D_1. A comparison of the max. O.D. of vanes of each impeller-runner determined by careful consideration of the above points, is shown in *Table 1*. Considering the stress concen-

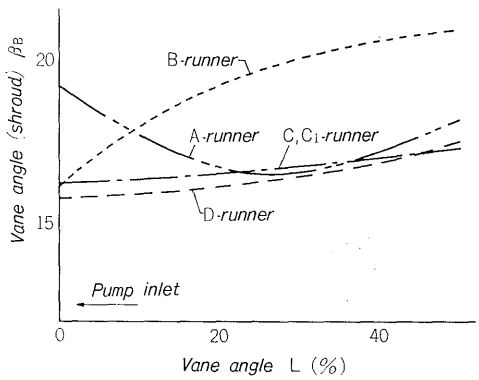

Fig. 14 vane angle distribution near shroud

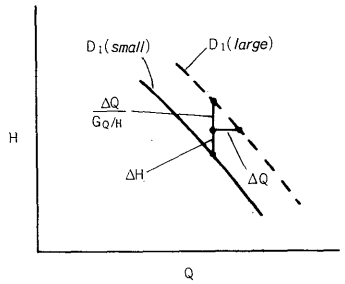

Fig. 15 Head rise resulting from increase of maximum O.D. of vane

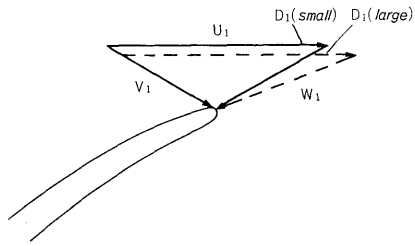

Fig. 16 Deflection of velocity triangle at turbine inlet with increase of maximum O.D. of vanes

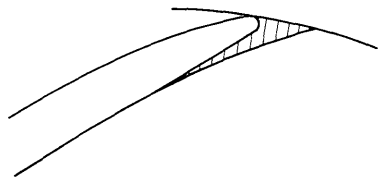

(a) Underfile

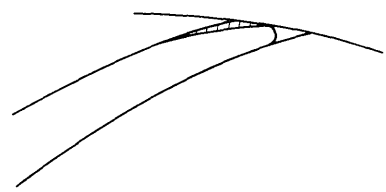

(b) Overfile

Fig. 17 Vane shape at pump discharge

tration at the junctures of vane with crown and shroud, the max. O.D. of the vanes of C_1-runner was limited by the max. O.D. of the crown and shroud.

(2) Vane outlet shape

It is well known that when the suction surface of the vane at the pump outlet is underfiled as shown in *Fig. 17* (a), the pump head is increased. This vane shape is also effective in suppressing cavitation on the suction surface of the bucket inlet at high head turbining. This underfiling was already used in the vane shape of the A-runner but since there was some inconsistency with the degree of underfiling from shroud to crown, the vane shapes of B~D-runners were layouted by Fuji computer program with careful consideration on the underfiling.

Conversely, when the pressure surface was overfiled as in *Fig. 17* (b), the pumping head was decreased somewhat but the separation of the flow from the pressure surface at low head turbining was suppressed and the variable head characteristics were improved which is an advantage for a reversible pump-turbine. Since the roundness of the bucket leading edge shape was small and the leading edge was rather sharp in the A-runner, the leading edge roundness was increased and blunt nose was adopted in the B~D-runners and improvement was made in consideration of the change of the flow angle (head variation).

These various design parameters mentioned above were imputed into the runner layout computer code developed by Fuji Electric and finally the optimum values for the vane profiles of runners B~D were obtained after the many design output from the computer. The core box drawings for wood patterns and template drawings for finishing were all automatically prepared by Fuji X-Y digital plotter program. The extremely smooth vane profile drawings were thus made very speedily and correctly without the risk of manual error. *Table 2* gives an outline of the special features of the impeller profiles of runners B~D.

Table 2 **Special feature of development runners**

Runner	Features
B	D_{2c}/D_3 is minimum. D_1 and shroud inner contour are same as A-runner.
C	D_{2c}/D_3 is somewhat larger than that of A-runner. D_1 is maximum Vane angle change along shroud of pump inlet is gradual. Shroud inner surface at pump inlet is inclined.
C_1	D_1 of C-runner is shortened to max. O.D. of shroud and crown
D	D_{2c}/D_3 is maximum. Otherwise similar to C-runner

2. Pump Performance

Fig. 18 shows the model pump test results for runners A, B, C, C_1 and D (values corresponding to the envelope of efficiency curves of the respective gate openings).

1) Discharge at beginning of back flow

Table 3 shows the results of measurement of discharge at the beginning of the back flow of each impeller. This discharge is largest in the B-runner which has the smallest D_{2c}/D_3. In accordance with this, the transition zone of the head-discharge curve due to stall at the pump inlet appears and the efficiency decreases with the large discharge. It was observed that back flow of B-runner first occurs on the shroud side and developed gradually to the crown side along with a decrease in the discharge.

On the other hand, the discharge at the beginning of back flow was the smallest in the D-runner which has the largest D_{2c}. Instead of suppression up to the smallest discharge once the back flow occurs with the decrease in discharge, there is almost complete back flow from shroud to crown. In the D-runner, the discharge at the point which the gradient of the head-discharge curve decrease is also the smallest and the head and efficiency are in creased at higher head. The back flow in the C and C_1-runners is just about between that of the B and D-runners and, as was described previously, the evident influence of D_{2c} on the back flow was confirmed experimentally.

2) Hydraulic pressure fluctuation

Table 3 shows the heads of the vibration peaks

Table 3 **Comparison of pump performance**

			A	B	C	C_1	D
Discharge at beginning of back flow	Q_{BF}/Q_{SF}	%	68.0	70.0	66.6	66.6	62.5
Head of vibration peak	$H_{\Delta Hmax}$	m	97	95	101	100	102
Increase of pump input power	$\Delta P_{H=95}$	%	—	1.0	16.6	9.6	12.4
Rise of pump efficiency	$\Delta\eta_{H=95}$	%	—	−2.3	4.6	3.2	4.6

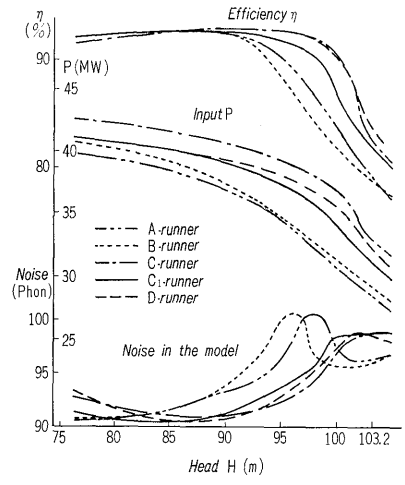

Fig. 18 Comparison of pump characteristics

for each impeller. In the D-runner, the shift was greatest to the higher head and the value for the C_1-runner was between those of the D and A-runners.

The D_1 of C_1-runner is 0.65% larger than that air A-runner. As mentioned in item 2) (1) of clause 1, the increment of head rise of C_1-runner in respect to A-runner becomes $\Delta H+\Delta Q/G_{Q/H}=1.3+1.3/2.7=1.8\%$.

On the other hand, the head of vibration peak in C_1-runner (100 m) was 3 m (3%) greater than that of A-runner (97 m). Therefore, since the 1.8 m (1.8%) in the above improvement of 3 m (3%) is resulted from the D_1 increase, the remaining 1.2 m (1.2%) should be attributed to the effect of D_{2c} increase and so on.

3) Cavitation

The cavitation developes on the suction surface of impeller vanes at pump inlet together with a decrease in the discharge, but since the B-runner has the largest discharge at the beginning of back flow, there is less chance to develope the cavitation and moreover since D_{2c} is small, there is almost no cavitation on the crown side and therefore, the cavitation characteristics are the best (*Fig. 19* (b)). On the other hand, since the D-runner has the smallest discharge at the beginning of back flow, there is more chance to develope the cavitation on the suction surface. However, because the vane angle of the pump inlet is reduced and the vane angle change rate along the stream-line is small, the degree of cavitation development is small at shroud side, cavitation on the crown side is rather developes first because of larger D_{2c} (*Fig. 19* (d)). Since the vane angle change rates of C and C_1-runners are approximately the same as that of D-runner and the D_{2c} values are almost midway between those of B and D-runners, the cavitation in C and C_1-runners is most uniform between crown and shroud (*Fig. 19* (c)) which reached the greatest improvement compared with the A-runner.

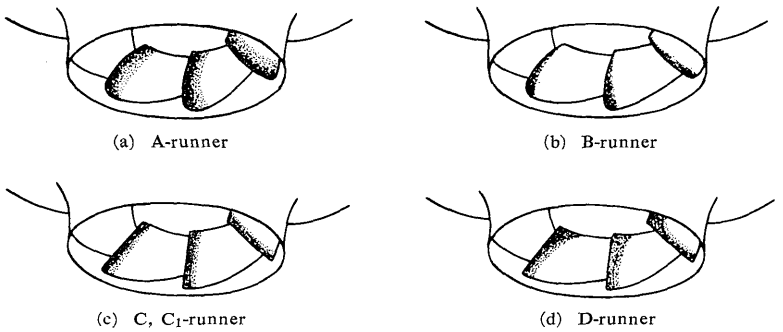

Fig. 19 Sketches of cavitation developed along suction surface of vane at pump inlet (H=90 m, σ=0.21)

4) Pump input power and efficiency

Table 3 shows the pump input power and efficiency of each impeller at $H=95$ m in comparison with the improved characteristics at higher heads. The effect is the greatest in the C and D-runners which have the largest vane outer diameters. These two are followed by the C_1-runner.

After a synthetic evaluation of pump performance was made from the above points, the C_1-runner was finally judged to be the best.

3. Turbine Performance

1) Efficiency

Table 4 **Comparison of turbine performance**

			A	B	C	C_1	D
Difference in optimum efficiency	$\eta_{max}-\eta_{max(A)}$	%	—	0.6	0.9	1.0	0.9
Beginning head of leading edge cavitation (suction surface)	H high	m	84	89	99	99	95
Beginning head of leading edge cavitation (pressure surface)	H low	m	69	71	74	73	74

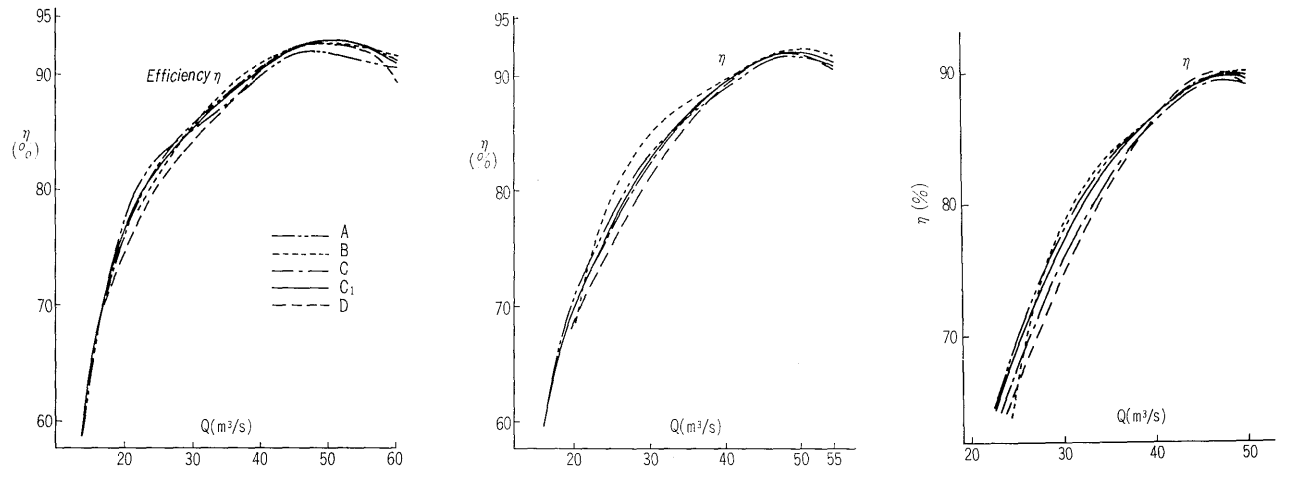

Fig. 20 Comparison of turbine efficiency

Fig. 20 shows the efficiency performance as turbine at maximum head (101.8 m), normal head (83.5 m) and lower head (70 m) from the results of the model tests. *Table 4* shows a comparison of maximum turbine efficiencies obtained. In the B-runner with the smallest D_{2c}, both full and partial load efficiencies showed the best and the so-called variable discharge performance was excellent. In the D-runner with the largest D_{2c}, conversely, the variable discharge performance deteriorated somewhat. In the case of the C and C_1-runners with D_{2c} values between those of the B and D-runners, the variable discharge performance was also midway between the two. If the efficiency of the C_1-runner is compared with that of the A-runner, it is improved at high heads but somewhat less at low heads (Table 5).

2) Bucket inlet cavitation

Table 4 shows the results of measurements of the heads at which cavitation noise from the suction surface of the bucket inlet as turbine begins at maximum wicket gate opening. It is evident that cavitation begins at higher heads from these values. The best characteristics are those of the C and C_1- runners with values toward high heads of approximately 15 m more than that for the A-runner.

Table 4 also shows the heads at which cavitation noise begins from the pressure surface of turbine inlet. Cavitation occurs at lower heads from these values. The A-runner had the best characteristics and the C_1-runner was 4 m more toward the higher heads.

Table 5 Comparison of turbine efficiency

$\eta_{c1}-\eta_A$	10MW	η_{max}	P_{FULL}
$\Delta\eta_{H=101.8}$	1.0	0.7	0.9
$\Delta\eta_{H=70}$	-1.3	-0.3	-0.3

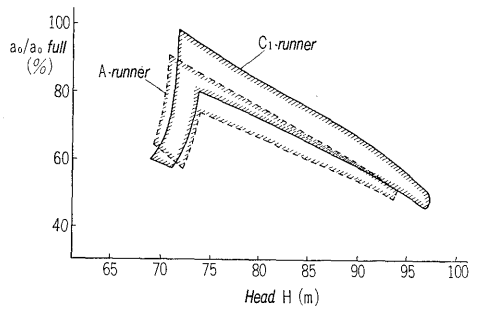

(a) Pumping

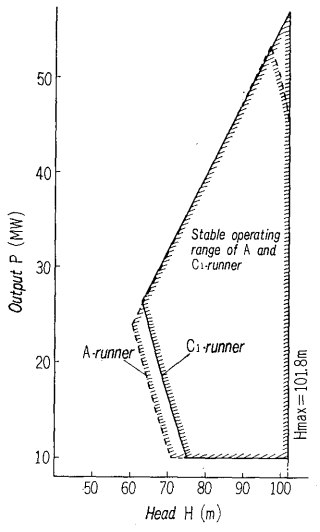

(b) Generating

Fig. 21 Stable operating range of A and C_1-runner

4. Stable Operating Range

As a result of careful investigations adding the above results to those of a stress analysis of the impeller-runner using the Fuji computer programs of finite element method, a synthetic evaluation was made and the C_1-impeller-runner was finally chosen. The stable pumping operating ranges for the C_1 and A-runners are shown in *Fig. 21* (a) and the stable generating ranges in *Fig. 21* (b). In order to determine the stable operating range of the C_1-runner, firstly the stable operating range obtained from past experience at the site were carefully compared with the results of model vibration tests on the A-runner and allowable values were established for the hydraulic pressure fluctuations, wicket gate hydraulic torque fluctuations, cavitation noise, variations of flow patterns by visual observations, etc. Then the stable operating range of the C_1-runner was determinied directly using these allowable values established for the A-runner.

5. Four Quadrant Characteristics

The four quadrant characteristics and their vibration characteristics do not change so much when only the impeller vane shape differs slightly if the pumptutbine specific speed and the stationary parts are fixed constant. The four quadrant characteristics of the C_1-runner are shown as an example in *Fig. 22*.

In order to suppress entrance to the reverse rpm pump zone where vibrations are large as much as possible after load rejection, the wicket gate closing speed should be increased and the gate opening from which closing speed is retarded should be raised as much as possible within the permissible ranges of pressure rise and speed rise. Using the four quadrant characteristics of the C_1-runner, load rejection characteristics were simulated for various conditions by Fuji computer program on transient analysis. *Fig. 23* shows an example of the results at the optimum wicket gate closing speed and *Fig. 22* shows the trace at load rejection. The max. values of wicket gate hydraulic opening torque and its fluctuations in the C_1-runner were much less than those in *Fig. 10* of the A-runner.

Since there is a problem of vibrations when the wicket gate opening is large in the small pump discharge and reverse flow pump ranges, it is advisable that the wicket gate closing speed at pump input power rejection also be high. *Fig. 24* shows an example of the computer results simulated and the

trace is shown in *Fig. 22*. The pressure drop presents no problem since the penstock is short at Hatanagi.

V. CONCLUSION

It is thought that there are no other similar case like that of the model tests on the A-runner where the model test were performed to prove the knowledge gained from the operating experience for 10 years at the site. It is highly significant that if the conditions are carefully selected and the observations carefully made in the model test, it has been found that it is possible to predict sufficiently the vibration phenomena in the prototype.

It was confirmed that under the great restriction that there be absolutely no change in the stationary parts, the pump and turbine performance and vibration characteristics of high head pumping and generating in a pump-turbine could be improved by changing only the impeller vane shape. Highly important experience for the progress of pump-turbine design techniques has been gained from this research and development.

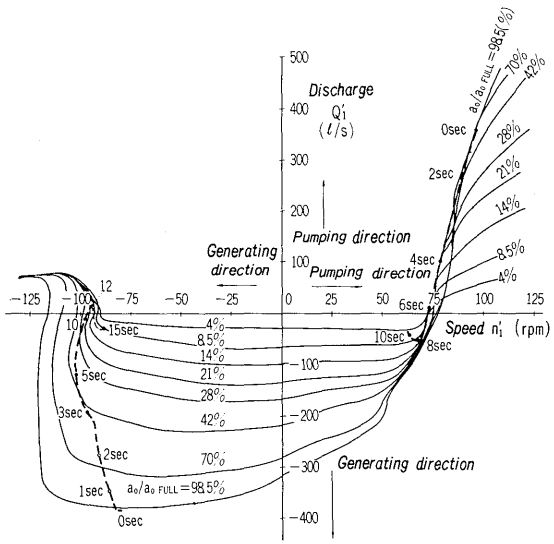

Fig. 22 Four quadrant characteristics of C_1-runner

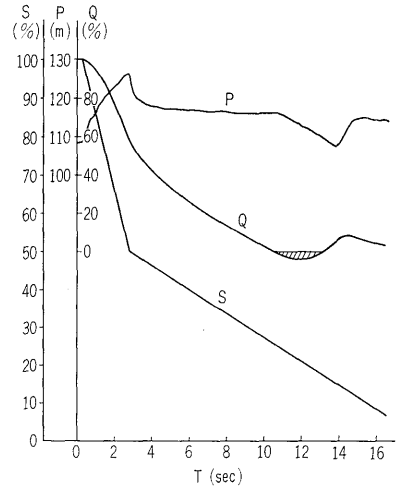

Fig. 23 Revised load rejection characteristics (C_1-runner)

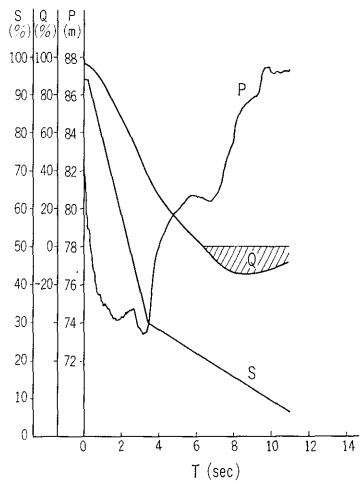

Fig. 24 Input power rejection characteristics (C_1-runner)

References :

(1) T. Kubota: Hydraulic Characteristics of Francis type pump-turbines (Japanese), Fuji Electric Journal, 40, No. 4, 1967

(2) T. Kubota and H. Matsui: Cavitation characteristics of forced vortex core in the flow of the Francis turbine Fuji Electric Review 18, No. 3, 1972

(3) Minami, Kawaguchi and Honma: Experiments concerning cavitation in centrifugal pumps (Japanese) J. of Jap. Soc. of Mech. Engineers, 62-485, 1959